RIS-Aided 6G Communication System With Accurate Traceable User Mobility

Peng Zhang, Jiayi Zhang 🔵 , *Senior Member, IEEE*, Huahua Xiao,
Hongyang Du 🔵 , *Graduate Student Member, IEEE*,
Dusit Niyato 🔵 , *Fellow, IEEE*, and Bo Ai 🔵 , *Fellow, IEEE*

Abstract—Reconfigurable intelligent surface (RIS) can effectively improve the performance of 6G communication systems by providing additional LoS paths. Although the beam alignment is necessary in 6G communication system due to the user mobility, the deployment of RIS increases significantly the complexity of beam tracking, making it impractical to apply directly conventional schemes. To this end, we study a time-varying RIS-aided millimeter wave (mmWave) system, a robust complex-valued extended Kalman filter method is proposed to tackle the beam alignment problem. More specifically, the proposed scheme achieves 17% performance gain compared to conventional training-based method. The impact of the number of RIS elements is investigated, there exists corresponding optimal number of RIS elements in terms of the minimum of the mean square error of the estimated beam angle. A simple but efficient algorithm to obtain the optimal number of RIS elements is presented. Simulation results demonstrate that, by employing the RIS in mmWave communication systems, the performance of beam tracking can be enhanced by 37% with proposed algorithms.

Index Terms—Beam tracking, reconfigurable intelligent surface, mmWave, mobility.

I. INTRODUCTION

It is foreseeable that the sixth generation (6G) communication system will utilize millimeter wave (mmWave) and/or terahertz (THz) bands to satisfy the increasing demand for data rate [1]. Because of the poor penetration of high frequency signals, 6G communication is heavily dependent on the existence of line-of-sight (LoS) paths to retain high-quality communication performance. However, when many obstacles, *e.g.*, urban buildings, exist in the communication system,

Peng Zhang, Jiayi Zhang, and Bo Ai are with the School of Electronic and Information Engineering, Beijing Jiaotong University, Beijing 100044, China, and also with the Frontiers Science Center for Smart High-speed Railway System, Beijing Jiaotong University, Beijing 100044, China (e-mail: 21120170@bjtu.edu.cn; jiayizhang@bjtu.edu.cn; boai@bjtu.edu.cn).

Huahua Xiao is with the ZTE Corporation, and State Key Laboratory of Mobile Network and Mobile Multimedia Technology, Shenzhen 518057, China (e-mail: xiao.huahua@zte.com.cn).

Hongyang Du and Dusit Niyato are with the School of Computer Science and Engineering, Nanyang Technological University, Singapore 639798 (e-mail: hongyang001@e.ntu.edu.sg; DNIYATO@ntu.edu.sg).

Digital Object Identifier 10.1109/TVT.2022.3214818

LoS paths cannot always be available. To this end, the reconfigurable intelligent surface (RIS) is introduced recently as an cost-effective and energy-efficient device to construct LoS paths for mmWave signals [2]. In general, RIS is a metamaterial surface with a large number of passive reflect elements. With the proper deployment of RIS, LoS paths between the transmitter and RIS, as well as those between the RIS and receiver, can be efficiently utilized. Thus, RIS provides a novel method to solve the wireless channel fading impairment and interference problems, and potentially offers huge gains compared with traditional wireless communications [3].

There are extensive literatures of RIS-aided mmWave communication systems, *e.g.*, [4], [5], [6], [7] and the references therein. It is shown that the use of the mmWave frequency band can provide high data rate in a variety of communication scenarios. However, the beams of mmWave signals are typically narrow, making it difficult to ensure alignment with mobile receivers [8]. While the RIS can provide additional LoS links, the deployment of RIS in mmWave systems further increases the difficulty of beam alignment [9]. To keep the alignment of the beam between the transceivers and maintain the existence of LoS paths, novel beam tracking schemes for the RIS-aided system need to be designed.

Conventional beam tracking schemes can be divided into two categories [10], [11], [12], [13], [14], [15]. The first one is the codebook-based scheme that has been employed widely in mmWave communications [10], [11]. Each codeword represent a possible beam direction. To select the best beam direction from the predefined codebook, the training process is typically performed between transceivers [12]. While the codebook-based scheme can track mobile users and resolve blocked LoS paths in slow time-varying systems, larger delays might exist when dealing with large antenna array systems. The second type of beam tracking scheme is dependent on the model of the user mobility. For example, the user mobility is assumed to follow the first-order Gauss-Markov model, and an Extended Kalman Filter (EKF) method is used to track the optimal beam [13]. To further enhance the accuracy of beam tracking, a kinematic model is employed to model the user mobility, and a modified unscented Kalman filter (UKF) is used to track precisely the channel beam [14]. Furthermore, a robust beam tracking algorithm using least mean square (LMS) and bidirectional LMS methods is proposed for mobile mmWave communication systems [15]. However, the designs discussed above are limited to end-to-end communication systems and high precision phase shifting of the RIS entails significant hardware costs.

To obtain the optimal beam direction in the RIS-aided system, it is necessary to design a beam tracking scheme that has low training cost and does not require complex channel estimation. To fill this research gap, we propose a robust complex-valued EKF method to design a beam tracking algorithm for the RIS-aided millimeter wave mobile system. The main contributions of this paper include:

- We study a time-varying RIS-aided mmWave communication system with a multi-antenna BS and an UE. We present a robust complex-valued EKF based beam tracking scheme and derive the Jacobian matrix of the measurement model.
- To investigate the performance of the proposed tracking algorithm, we present a comparsion to conventional training-based method, achieving 17% performance gain. We employ mean square error (MSE) to study the impacts of the number of RIS elements N_{RIS}. We propose a simple but efficient algorithm to obtain N_{RIS}^{opt} with different values of SNR and process noise to minimize the MSE. It is shown that the performance can be
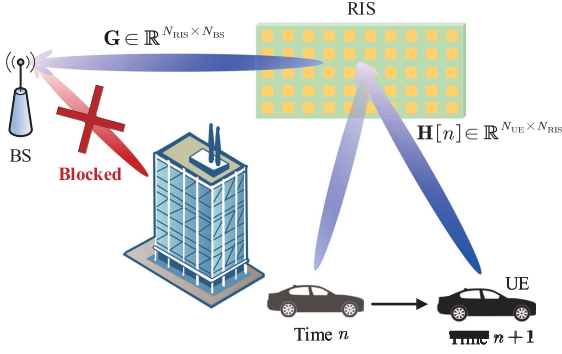
Fig. 1. System diagram of RIS-aided mmWave communication system.

improved by 37% compared with the mmWave system without RIS [13].

Notations: Boldface lower-case and capital letters represent column vectors and matrices, respectively. $(\cdot)^{\mathrm{T}}$ and $(\cdot)^{\mathrm{H}}$ denote the transpose and transpose-conjugate operation, respectively. $\mathbb{E}$ represents statistical expectation, $\mathbb{C}$ denotes the set of complex numbers, $\mathbf{I}_N$ is the $N \times N$ size identity matrix, $[\mathbf{a}]_i$ denote the i-th element of vector $\mathbf{a}$ and $[\mathbf{A}]_{i,j}$ represent the (i,j)-th element of matrix $\mathbf{A}$.

II. SYSTEM MODEL

We consider a time-varying mmWave system in Fig. 1. An N_{BS}-antenna BS transmits signals to an N_{UE}-antenna UE with the aid of an N_{RIS} reflect elements RIS. We consider that the LoS path is blocked [16]. At time slot n, the received signal at UE is given by

$$\mathbf{y}[n] = \mathbf{H}[n]\,\boldsymbol{\Theta}\mathbf{G}\mathbf{s} + \mathbf{w}, \tag{1}$$

where $\mathbf{s} \in \mathbb{C}^{N_{\mathrm{BS}} \times 1}$ are the transmitted symbols with $\mathbb{E}\{\mathbf{s}^{\mathrm{H}}\mathbf{s}\} = 1$, $\mathbf{G} \in \mathbb{C}^{N_{\mathrm{RIS}} \times N_{\mathrm{BS}}}$ is the channel between the BS and the RIS, $\mathbf{H}[n] \in \mathbb{C}^{N_{\mathrm{UE}} \times N_{\mathrm{RIS}}}$ is the channel between the RIS and the UE at time slot n, $\boldsymbol{\Theta} = \mathrm{diag}\{e^{\mathrm{j}\phi_1}, e^{\mathrm{j}\phi_2}, \ldots, e^{\mathrm{j}\phi_{N_{\mathrm{RIS}}}}\} \in \mathbb{C}^{N_{\mathrm{RIS}} \times N_{\mathrm{RIS}}}$ is the diagonal reflect matrix of the RIS, $\phi_n \in [0, 2\pi)$ is the phase shift of the n-th reflecting element, and $\mathbf{w} \sim \mathcal{CN}(\mathbf{0}, \mathbf{I}_{N_{\mathrm{UE}}}) \in \mathbb{C}^{N_{\mathrm{UE}} \times 1}$ is the additive white Gaussian noise.

We consider that the antenna arrays of the BS, the RIS and the UE are uniform linear arrays (ULA). Meanwhile, the mmWave channel is commonly assumed to be sparse [13]. The sparsity of the channel allows different multipaths to be separated from each other, and only one path is in the main beam direction, while the other paths are considered to be in the side lobe direction. Tracking a single path allows beam alignment between the transceivers, and the tracking algorithm can be similarly extended to tracking multiple paths. For simplicity, the channel model with a single main path is employed. The general multi-path channel model can be obtained from the angle-of-arrival (AoA) and the angle-of-departure (AoD) of the main path [16]. The channel state information between the BS and the RIS is known, since the locations of both the BS and the RIS are fixed. Specifically, we can express the BS-RIS and the RIS-UE channel as

$$\mathbf{G} = \rho_g \mathbf{a}(\theta_g)\,\mathbf{a}^{\mathrm{H}}(\phi_g), \tag{2}$$

$$\mathbf{H}[n] = \rho_h[n]\,\mathbf{a}(\theta_h[n])\,\mathbf{a}^{\mathrm{H}}(\phi_h[n]), \tag{3}$$

respectively, where ρ_g and $\rho_h[n]$ are channel coefficients. Steering vectors of the corresponding channels are given as

$$[\mathbf{a}(\theta_g)]_i = \frac{1}{\sqrt{N_{\mathrm{RIS}}}} e^{\mathrm{j}\frac{2\pi}{\lambda} d_{\mathrm{RIS}}(i-1)\cos(\theta_g)}, \tag{4a}$$

$$[\mathbf{a}(\phi_g)]_j = \frac{1}{\sqrt{N_{\mathrm{BS}}}} e^{\mathrm{j}\frac{2\pi}{\lambda} d_{\mathrm{BS}}(j-1)\cos(\phi_g)}, \tag{4b}$$

$$[\mathbf{a}(\theta_h[n])]_k = \frac{1}{\sqrt{N_{\mathrm{UE}}}} e^{\mathrm{j}\frac{2\pi}{\lambda} d_{\mathrm{UE}}(k-1)\cos(\theta_h[n])}, \tag{4c}$$

$$[\mathbf{a}(\phi_h[n])]_i = \frac{1}{\sqrt{N_{\mathrm{RIS}}}} e^{\mathrm{j}\frac{2\pi}{\lambda} d_{\mathrm{RIS}}(i-1)\cos(\phi_h[n])}, \tag{4d}$$

where λ is the wavelength, $i \in \{1, \ldots, N_{\mathrm{RIS}}\}$, $j \in \{1, \ldots, N_{\mathrm{BS}}\}$, and $k \in \{1, \ldots, N_{\mathrm{UE}}\}$ denote the element indexes of respective steering vectors, θ_g, ϕ_g, $\theta_h[n]$ and $\phi_h[n]$ are the AoA of RIS, AoD of BS, AoA of UE and AoD of RIS, respectively. d_{BS}, d_{RIS} and d_{UE} are antenna spacing of BS, RIS and UE, respectively.

A. Single-Antenna UE Case

A special case of a single antenna UE can obtain meaningful insights, *e.g.*, the optimal RIS configuration. Meanwhile, the algorithm proposed in this paper is suitable for any number of antennas. We consider that the N_{BS}-antenna BS transmits signal to a single-antenna UE through beamformer $\mathbf{f} \in \mathbb{C}^{N_{\mathrm{BS}} \times 1}$. The received signal at UE can be rewritten as

$$y[n] = \alpha[n]\,\mathbf{a}^{\mathrm{H}}(\phi_h[n])\,\boldsymbol{\Theta}\mathbf{a}(\theta_g)\,\mathbf{a}^{\mathrm{H}}(\phi_g)\,\mathbf{f}s + w \in \mathbb{C}, \tag{5}$$

where $\alpha[n] \triangleq \rho_g \rho_h[n]$ is the composition channel coefficient of the BS-RIS-UE channel, $w \sim \mathcal{CN}(0, \sigma_w^2)$ is the additive white Gaussian noise, and σ_w is the variance of the noise. We consider that $\mathbf{f} = \mathbf{a}(\phi_g)/|\mathbf{a}(\phi_g)|$. The AoD of the BS can be obtained by AoD estimation algorithms [10]. The received signal can be written as

$$y[n] = \frac{\alpha[n]}{\sqrt{N_{\mathrm{RIS}}}} \sum_{\ell=1}^{N_{\mathrm{RIS}}} e^{\mathrm{j}\left[\phi_\ell - \frac{2\pi}{\lambda} d_{\mathrm{RIS}}(\ell-1)\left(\cos(\phi_h[n]) - \cos(\theta_g)\right)\right]} s + w. \tag{6}$$

At time slot n, the optimal RIS configuration can be obtained by maximizing the received SNR, *i.e.*,

$$\boldsymbol{\Theta}_{\mathrm{opt}} = \arg\max \left| \frac{\alpha[n]\,\mathbf{a}^{\mathrm{H}}(\phi_h[n])\,\boldsymbol{\Theta}\mathbf{a}(\theta_g)\,\mathbf{a}^{\mathrm{H}}(\phi_g)\,\mathbf{f}}{\sigma_w^2} \right|^2. \tag{7}$$

Substituting (6) into (7), the optimal configuration of ℓ-th principal diagonal element of RIS matrix can be given as

$$\phi_\ell = \frac{2\pi}{\lambda} d_{\mathrm{RIS}}(\ell-1)\left(\cos(\phi_h[n]) - \cos(\theta_g)\right), \tag{8}$$

where $\ell \in \{1, 2, \ldots, N_{\mathrm{RIS}}\}$.

III. BEAM TRACKING ALGORITHM

We apply the EKF in our beam tracking algorithm, because the EKF can provide excellent performance for nonlinear estimation with low complexity. The EKF operates in a "predict-update" loop. After receiveing the signal as expressed in (1), the EKF updates the estimate and the uncertainty of the current state with the received signal. We consider that an AoA/AoD estimator is used at the starting point to output estimates for the proposed beam tracking algorithm. The optimal initial RIS configuration $\boldsymbol{\Theta}_{\mathrm{opt}}[1]$ can be obtained using (8).

A. State Evolution Model and Measurement Model

The state vector is defined by

$$\mathbf{x}[n] = [\Re(\alpha[n]), \Im(\alpha[n]), \phi_h[n], \theta_h[n]]^{\mathrm{T}}, \tag{9}$$

where $\alpha[n] = \Re(\alpha[n]) + \mathrm{j}\Im(\alpha[n])$ is the composition channel coefficient of the BS-RIS-UE channel. We consider that $\alpha[n]$ follows the

first-order Gauss-Markov model, the state extrapolation model of is $\alpha[n]$ given by

$$\alpha [n + 1] = \rho\alpha [n] + \zeta [n], \tag{10}$$

where ρ is the correlation coefficient, $\zeta[n] \sim \mathcal{CN}(0, 1 - \rho^2)$, and $\alpha[0] \sim \mathcal{CN}(0, 1)$. We assume that a common extrapolation model for the AoA/AoD is followed by a Gaussian process noise and the AoA and AoD are independent of each other and $\alpha[n]$. The state evolution model can be written as

$$\boldsymbol{x} [n] = \mathbf{F}\boldsymbol{x} [n - 1] + \boldsymbol{u} [n - 1], \tag{11}$$

where $\mathbf{F} = \mathrm{diag}\{\rho, \rho, 1, 1\}, \boldsymbol{u}[n] \sim \mathcal{CN}(\mathbf{0}, \boldsymbol{\Sigma_u})$ with $\boldsymbol{\Sigma_u} = \mathrm{diag}\{1 - \rho^2, 1 - \rho^2, \sigma_\theta^2, \sigma_\phi^2\}, \sigma_\phi^2$ and σ_θ^2 are the variance of the Gaussian process noise.

The measurement model can be represented by the received signal $\mathbf{y}[k]$ as

$$\mathbf{y} [k] = \mathbf{h} (\boldsymbol{x} [k]) + \mathbf{w}. \tag{12}$$

B. Robust Complex-Valued EKF Algorithm

Since the real and complex mixed numbers will make the algorithm stop working and inaccurate when encountering singular matrices. Therefore, we extended and adjusted each iteration to improve the stability and accuracy. After deriving the state evolution model and measurement model, the robust complex-valued EKF recursion is given as

$$\hat{\boldsymbol{x}} [n|n - 1] = \mathbf{F}\hat{\boldsymbol{x}} [n - 1|n - 1], \tag{13a}$$

$$\mathbf{K}_n = \mathbf{P}_{n|n-1}\tilde{\mathbf{J}}_k^{\mathrm{T}} \left(\tilde{\mathbf{J}}_n \mathbf{P}_{n|n-1}\tilde{\mathbf{J}}_n^{\mathrm{T}}\right)^{-1}, \tag{13b}$$

$$\hat{\boldsymbol{x}} [n|n] = \hat{\boldsymbol{x}} [n|n - 1] + \mathbf{K}_n \left\{\tilde{\mathbf{y}} [n] - \mathbf{h}(\hat{\boldsymbol{x}} [n|n - 1])\right\}, \tag{13c}$$

$$\mathbf{P}_{n|n} = \left(\mathbf{I} - \mathbf{K}_n\tilde{\mathbf{J}}_n\right) \mathbf{P}_{n|n-1}, \tag{13d}$$

$$\mathbf{P}_{n+1|n} = \mathbf{F}\mathbf{P}_{n|n}\mathbf{F}^{\mathrm{T}} + \mathbf{Q}_n, \tag{13e}$$

where $\tilde{\mathbf{y}}[n] = [\Re(\mathbf{y}[n]), \Im(\mathbf{y}[n])]$, $\tilde{\mathbf{J}}_n = [\Re(\mathbf{J}_n), \Im(\mathbf{J}_n)]$ with $\mathbf{J}_n = \Delta_{\boldsymbol{x}}\mathbf{h}|_{\boldsymbol{x} = \hat{\boldsymbol{x}}[n|n-1]}$ which is the Jacobian matrix of measurement model. Assuming that $\hat{\boldsymbol{x}}[1|0] = \hat{\boldsymbol{x}}_0$, $\mathbf{P}_{1|0} = \boldsymbol{\Sigma_u}$, and $\mathbf{Q}_n = \boldsymbol{\Sigma_u}$ does not change with time, where $\hat{\boldsymbol{x}}_0$ is the estimate from the AoA/AoD estimator.

The total required signaling of the proposed scheme at each iteration has N_{UE} symbols. Besides, the complexity of Kalman filter is known to be $\mathcal{O}(N_{\mathrm{UE}}^3)$ [17], and the function $\mathcal{O}(\mathbf{h}(\boldsymbol{x}[n]))$ could affect the complexity in EKF. Overall, the complexity of the whole proposed algorithm can be expressed as $\max(\mathcal{O}(N_{\mathrm{RIS}}^2(N_{\mathrm{BS}} + N_{\mathrm{UE}})), \mathcal{O}(N_{\mathrm{UE}}^3))$.

C. Jacobian Matrix

The measurement model in (12) can be written as

$$\mathbf{h} (\boldsymbol{x} [n]) = \mathbf{H} [n]\,\boldsymbol{\Theta}\mathbf{G}\mathbf{s}$$

$$= \alpha [n]\, \mathbf{a} (\theta_h [n])\, \mathbf{a}^{\mathrm{H}} (\phi_h [n])\, \mathbf{G}_{\mathrm{eff}}, \tag{14}$$

where $\alpha[n] \triangleq \rho_g \rho_h[n]$ is the composition channel coefficient of BS-RIS-UE channel. For the convenience of representing and calculating the Jacobian matrix, let $\mathbf{G}_{\mathrm{eff}} \triangleq \boldsymbol{\Theta}\mathbf{a}(\theta_g)\mathbf{a}^{\mathrm{H}}(\phi_g)$.

The Jacobian matrix of $\mathbf{h}$ is defined as an $N_{\mathrm{UE}} \times 4$ matrix as

$$\mathbf{J} = \Delta_{\boldsymbol{x}}\mathbf{h} = \left[\frac{\partial \mathbf{h}}{\partial \Re(\alpha [n])}, \frac{\partial \mathbf{h}}{\partial \Im(\alpha [n])}, \frac{\partial \mathbf{h}}{\partial \phi_h [n]}, \frac{\partial \mathbf{h}}{\partial \theta_h [n]}\right]. \tag{15}$$

Algorithm 1: Algorithm for Optimal Number of RIS Elements.

Input: Minimum number of RIS elements $N_{\mathrm{RIS}}^{\mathrm{min}}$, maximum number of RIS elements $N_{\mathrm{RIS}}^{\mathrm{max}}$, initial number of RIS elements $N_{\mathrm{RIS}}^{\mathrm{init}}$ and covariance vector $\mathbf{p} \in \mathbb{R}^{1 \times 2}$.

$\quad N_{\mathrm{RIS}}^{\mathrm{opt}} = N_{\mathrm{RIS}}^{\mathrm{init}}$,
$\quad$ **while** $N_{\mathrm{RIS}}^{\mathrm{min}} \neq N_{\mathrm{RIS}}^{\mathrm{max}}$ **do**
$\qquad$ **for** $N_{\mathrm{RIS}} = N_{\mathrm{RIS}}^{\mathrm{opt}} : N_{\mathrm{RIS}}^{\mathrm{opt}} + 1$ **do**
$\qquad\quad$ **for** $n = 1 : N_{\mathrm{slot}}$ **do**
$\qquad\qquad$ (13a), (13b), (13c), (13d),
$\qquad\qquad$ index $= N_{\mathrm{RIS}} \bmod N_{\mathrm{RIS}}^{\mathrm{opt}}$,
$\qquad\qquad [\mathbf{p}]_{(\mathrm{index})+1} \leftarrow [\mathbf{p}]_{(\mathrm{index})+1} + \frac{1}{N_{\mathrm{slot}}}[\mathbf{P}_{n|n}]_{3,3}$,
$\qquad\qquad$ (13e),
$\qquad\quad$ **end for**
$\qquad$ **end for**
$\qquad$ **if** $[\mathbf{p}]_{(N_{\mathrm{RIS}}+1 \bmod N_{\mathrm{RIS}}^{\mathrm{opt}})+1} > [\mathbf{p}]_{(N_{\mathrm{RIS}} \bmod N_{\mathrm{RIS}}^{\mathrm{opt}})+1}$ **then**
$\qquad\quad N_{\mathrm{RIS}}^{\mathrm{min}} = N_{\mathrm{RIS}}^{\mathrm{opt}}, N_{\mathrm{RIS}}^{\mathrm{opt}} \leftarrow \lfloor\frac{N_{\mathrm{RIS}}^{\mathrm{opt}}+1}{2}\rfloor$,
$\qquad$ **else**
$\qquad\quad N_{\mathrm{RIS}}^{\mathrm{max}} = N_{\mathrm{RIS}}^{\mathrm{opt}}, N_{\mathrm{RIS}}^{\mathrm{opt}} \leftarrow \lfloor\frac{N_{\mathrm{RIS}}^{\mathrm{opt}}+N_{\mathrm{RIS}}^{\mathrm{max}}}{2}\rfloor$,
$\qquad$ **end if**
$\quad$ **end while**
Output: $N_{\mathrm{RIS}}^{\mathrm{opt}}$.

Substituting (14) into (15), the Jacobian matrix of $\mathbf{h}$ can be obtained as

$$\mathbf{J} = \begin{bmatrix} \mathbf{a} (\theta_h [n])\, \mathbf{a}^{\mathrm{H}} (\phi_h [n])\, \mathbf{G}_{\mathrm{eff}} \\ \mathbf{j}\mathbf{a} (\theta_h [n])\, \mathbf{a}^{\mathrm{H}} (\phi_h [n])\, \mathbf{G}_{\mathrm{eff}} \\ \alpha [n]\, \mathbf{a} (\theta_h [n])\, \frac{\partial \mathbf{a}^{\mathrm{H}}(\phi_h [n])}{\partial \phi_h [n]}\, \mathbf{G}_{\mathrm{eff}} \\ \alpha [n]\, \frac{\partial \mathbf{a}(\theta_h [n])}{\partial \theta_h [n]}\, \mathbf{a}^{\mathrm{H}} (\phi_h [n])\, \mathbf{G}_{\mathrm{eff}} \end{bmatrix}^{\mathrm{T}}, \tag{16}$$

where

$$\left[\frac{\partial \mathbf{a}^{\mathrm{H}} (\phi_h [n])}{\partial \phi_h [n]}\right]_i = \frac{i - 1}{\sqrt{N_{\mathrm{RIS}}}}\frac{2\pi}{\lambda}d_{\mathrm{RIS}}\sin\phi_h [n]\left[\mathbf{a}^{\mathrm{H}} (\phi_h [n])\right]_i, \tag{17a}$$

$$\left[\frac{\partial \mathbf{a} (\theta_h [n])}{\partial \theta_h [n]}\right]_k = -\frac{k - 1}{\sqrt{N_{\mathrm{UE}}}}\frac{2\pi}{\lambda}d_{\mathrm{UE}}\sin\theta_h [n]\left[\mathbf{a} (\theta_h [n])\right]_k, \tag{17b}$$

where $i \in \{1, \ldots, N_{\mathrm{RIS}}\}$ and $k \in \{1, \ldots, N_{\mathrm{UE}}\}$ denote the elements index of steering vectors in (17a) and (17b), respectively.

D. Optimal Number of RIS Elements

There exists corresponding optimal number of RIS elements $N_{\mathrm{RIS}}^{\mathrm{opt}}$ for the proposed algorithm to implement optimal performance with different mmWave channel states. The optimal number of RIS elements is defined as the number of RIS elements that minimizes the mean square error (MSE) of average time slot, which is given by

$$N_{\mathrm{RIS}}^{\mathrm{opt}} = \arg\min \frac{1}{N_{\mathrm{slot}}}\sum_{n=1}^{N_{\mathrm{slot}}} \mathbb{E}\left[\left|\hat{\phi}_h [n] - \phi_h [n]\right|^2\right], \tag{18}$$

where N_{slot} is the number of time slots. Optimization based on binary search tree in [4] is given in Algorithm 1.

IV. NUMERICAL RESULTS AND DISCUSSION

Numerical investigations of the performance of the proposed tracking algorithms are shown in this section. The MSE of estimated angle
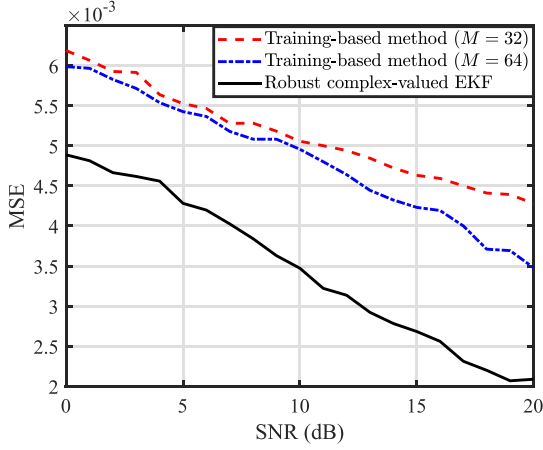
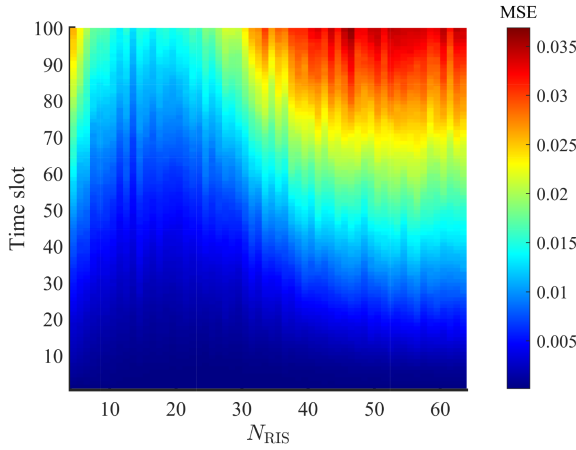Fig. 2. Comparsion of MSE of proposed scheme with training-based method versus different SNRs.

Fig. 3. MSE of AoD versus each time slot at SNR = 0 dB with different number of RIS elements.

is defined by $\text{MSE}[n] = \mathbb{E}[|\hat{\phi}_h[n] - \phi_h[n]|^2]$. Each MSE curve is obtained by averaging over 10^3 Monte-Carlo simulation loops. If not mentioned again, we set that $N_{BS} = N_{RIS} = 16$, $N_{UE} = 1$, the initial AoD is $45°$, $\rho = 0.995$, and $\sigma_\phi^2 = (0.5°)^2$. The impact of SNR, the number of RIS elements, and the comparison of mmWave mobility systems with and without RIS [13] are considered.

A. Comparsion to Conventional Training-Based Method

The comparsion of MSE performance between the proposed scheme and training-based at different SNRs is shown in Fig. 2. Assuming that M training beams uniformly distributed in directions are transimitted in beam training step, the one with the highest received signal power will be selected. It is noticed that the proposed scheme achieves 17% performance gain in MSE compared to the conventional training-based method. The reason is that, with the angle variation caused by mobility, more time is allocated to beam training step to track alignment, which increases the AoD estimation error.

B. Impact of the Number of RIS Elements

Fig. 3 shows the MSE of AoD at SNR of 0 dB. With the increase of the number of RIS elements, the performance of MSE is not improved as expected. However, when a larger number of RIS elements, i.e.,
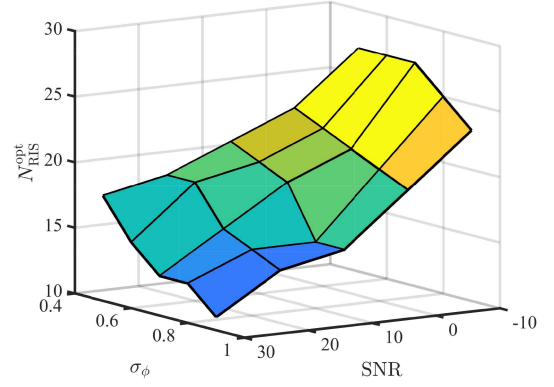

Fig. 4. Optimal number of RIS elements with different σ_ϕ^2 and SNRs.

$N_{RIS} = 64$, is configured, MSE performance is even worse than that of $N_{RIS} = 4$. The reason is that the beams get narrower due to large number of RIS elements, e.g., N_{RIS} is greater than 16, which make the change in the AoA/AoD becomes more sensitive to the changes in AoA/AoD. However, while the beam become narrow enough as in the $N_{RIS} = 64$, the AoA/AoD is out of the range of alignment due to the Gaussian process noise, which causes a poor tracking performance, i.e., the increase of MSE. Small number of RIS elements, e.g., N_{RIS} is less than 16, is not sensitive enough to track the change of the Gaussian process noise, while a large value of N_{RIS} causes misalignment during the signal transmission.

C. Optimal Number of RIS Elements

N_{RIS}^{opt} versus different σ_ϕ^2 and SNR is shown in Fig. 4. In this simulation, it is assumed that $N_{slot} = 100$, $N_{RIS}^{min} = 1$, $N_{RIS}^{max} = 128$ and $N_{RIS}^{init} = 64$. As the SNR increases, the optimal number of RIS elements becomes smaller, since increasing the SNR can significantly improve the mmWave channel conditions, and thus enhance the performance. As the Gaussian process noise variance σ_ϕ^2 increases from $(0.5°)^2$ to $(1°)^2$, the optimal number of RIS elements becomes smaller. However, an accurate algorithm step is more difficult to be implemented. The reason is that the mmWave channel becomes hostile, a wider beam is needed to cover the range of AoD changes. The wide beam will weaken the LoS path of the mmWave channel between transceivers. Blindly improving the performance may lead to the degradation of the performance of the mmWave communication system.

D. Comparison to Prior Work in [13]

Fig. 5 shows the comparison of the performance between the RIS-aided mmWave system and the mmWave system without RIS [13] at SNR = 0 dB with different Gaussian process noise. It is shown that the RIS-aided mmWave mobility system has 37% smaller MSE during the transmission time slots than no RIS system. With the assistance of RIS, the channel condition between the BS and the UE is improved, while the performance of the EKF is enhanced. Moreover, it is noticed that, as the Gaussian process noise variance is small, i.e., $\sigma_\phi^2 = (0.25°)^2$, the gap between the two curves becomes tight, the reason is that as the angle change is not so drastic, the two systems have similar performance.

V. CONCLUSION

In this paper, we studied an RIS-aided mmWave mobility system. A robust complex-valued EKF scheme was employed to implement the
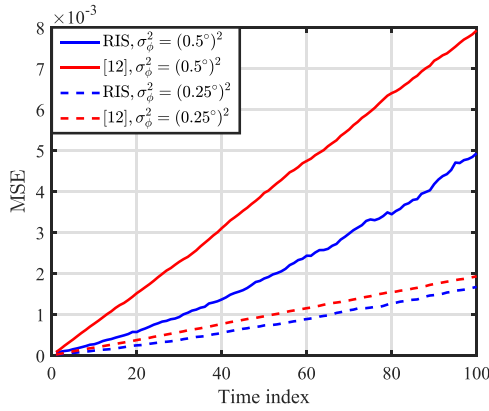
Fig. 5. Tracking performance of the mmWave system with and without RIS.

beam tracking algorithm and the Jacobian matrix of the measurement model was derived. We investigated that the proposed scheme achieved 17% performance gain compared with conventional training-based method. The impacts of the number of RIS elements was explored. We showed that there existed corresponding optimal number of RIS elements to minimize the MSE of the calculated angle for different mmWave channel conditions. Moreover, the optimal number of RIS elements were quantified with different SNRs. By comparing the mobile mmWave system with or without RIS, we found that RIS improved significantly the beam tracking performance by 37%.

REFERENCES

[1] Y. Zhu, B. Mao, Y. Kawamoto, and N. Kato, "Intelligent reflecting surface-aided vehicular networks toward 6G: Vision, proposal, and future directions," *IEEE Veh. Technol. Mag.*, vol. 16, no. 4, pp. 48–56, Dec. 2021.
[2] J. Zhang, E. Björnson, M. Matthaiou, D. W. K. Ng, H. Yang, and D. J. Love, "Prospective multiple antenna technologies for beyond 5G," *IEEE J. Sel. Areas Commun.*, vol. 38, no. 8, pp. 1637–1660, Aug. 2020.
[3] Q. Wu, S. Zhang, B. Zheng, C. You, and R. Zhang, "Intelligent reflecting surface-aided wireless communications: A tutorial," *IEEE Trans. Commun.*, vol. 69, no. 5, pp. 3313–3351, May 2021.
[4] H. Du, J. Zhang, J. Cheng, and B. Ai, "Millimeter wave communications with reconfigurable intelligent surfaces: Performance analysis and optimization," *IEEE Trans. Commun.*, vol. 69, no. 4, pp. 2752–2768, Apr. 2021.
[5] H. Hashida, Y. Kawamoto, N. Kato, M. Iwabuchi, and T. Murakami, "Mobility-aware user association strategy for IRS-aided mm-wave multi-beam transmission towards 6G," *IEEE J. Sel. Areas Commun.*, vol. 40, no. 5, pp. 1667–1678, May 2022.
[6] J. Zhao, L. Yu, K. Cai, Y. Zhu, and Z. Han, "RIS-aided ground-aerial NOMA communications: A distributionally robust DRL approach," *IEEE J. Sel. Areas Commun.*, vol. 40, no. 4, pp. 1287–1301, Apr. 2022.
[7] J. Zhang et al., "RIS-aided next-generation high-speed train communications: Challenges, solutions, and future directions," *IEEE Wireless Commun.*, vol. 28, no. 6, pp. 145–151, Dec. 2021.
[8] M. S. Elbamby, C. Perfecto, M. Bennis, and K. Doppler, "Toward low-latency and ultra-reliable virtual reality," *IEEE Netw.*, vol. 32, no. 2, pp. 78–84, Mar./Apr. 2018.
[9] Y. Zhang, J. Zhang, M. D. Renzo, H. Xiao, and B. Ai, "Reconfigurable intelligent surfaces with outdated channel state information: Centralized vs. distributed deployments," *IEEE Trans. Commun.*, vol. 70, no. 4, pp. 2742–2756, Apr. 2022.
[10] S. Hur, T. Kim, D. J. Love, J. V. Krogmeier, T. A. Thomas, and A. Ghosh, "Millimeter wave beamforming for wireless backhaul and access in small cell networks," *IEEE Trans. Commun.*, vol. 61, no. 10, pp. 4391–4403, Oct. 2013.
[11] D. Zhu, J. Choi, Q. Cheng, W. Xiao, and R. W. Heath, "High-resolution angle tracking for mobile wideband millimeter-wave systems with antenna array calibration," *IEEE Trans. Wireless Commun.*, vol. 17, no. 11, pp. 7173–7189, Nov. 2018.
[12] S. Noh, M. D. Zoltowski, and D. J. Love, "Multi-resolution codebook and adaptive beamforming sequence design for millimeter wave beam alignment," *IEEE Trans. Wireless Commun.*, vol. 16, no. 9, pp. 5689–5701, Sep. 2017.
[13] V. Va, H. Vikalo, and R. W. Heath, "Beam tracking for mobile millimeter wave communication systems," in *Proc. IEEE Glob. Conf. Signal Inf. Process.*, 2016, pp. 743–747.
[14] J. Zhao, F. Gao, W. Jia, S. Zhang, S. Jin, and H. Lin, "Angle domain hybrid precoding and channel tracking for millimeter wave massive MIMO systems," *IEEE Trans. Wireless Commun.*, vol. 16, no. 10, pp. 6868–6880, Oct. 2017.
[15] Y. Yapıcı and I. Güvenç, "Low-complexity adaptive beam and channel tracking for mobile mmwave communications," in *Proc. 52nd Asilomar Conf. Signals, Syst., Comput.*, 2018, pp. 572–576.
[16] X. Yang, C.-K. Wen, and S. Jin, "MIMO detection for reconfigurable intelligent surface-assisted millimeter wave systems," *IEEE J. Sel. Areas Commun.*, vol. 38, no. 8, pp. 1777–1792, Aug. 2020.
[17] V. Vaidehi and C. N. Krishnan, "Computational complexity of the Kalman tracking algorithm," *IETE J. Res.*, vol. 44, no. 3, pp. 125–134, Mar. 1998.